

**Wide Thermal Hysteresis for the Mononuclear Spin-Crossover Compound**  
***cis*-Bis(thiocyanato)bis[*N*-(2'-pyridylmethylene)-4-(phenylethynyl)anilino]iron(II)**

Jean-François Létard,<sup>†</sup> Philippe Guionneau,<sup>†</sup>  
 Epiphane Codjovi,<sup>†</sup> Olivier Lavastre,<sup>‡</sup> Georges Bravic,<sup>†</sup>  
 Daniel Chasseau,<sup>†</sup> and Olivier Kahn<sup>\*,†</sup>

Laboratoire des Sciences Moléculaires, Institut de  
 Chimie de la Matière Condensée de Bordeaux  
 UPR CNRS n°9048, 33608 Pessac Cedex, France  
 Laboratoire de Chimie de Coordination Organique  
 Université de Rennes I, Campus de Beaulieu  
 35042 Rennes, France

Received July 21, 1997

The most spectacular example of molecular bistability is probably offered by the spin-crossover phenomenon. Some  $d^n$ , with  $n = 4$  to 7, first-row transition metal ions in octahedral surroundings may exhibit a crossover between low-spin (LS) and high-spin (HS) states.<sup>1</sup> To a first approximation, this situation occurs when the quantum mechanical energy of the LS state in its equilibrium geometry is slightly lower than the quantum mechanical energy of the HS state, also in its equilibrium energy. Above a certain temperature, the thermodynamically stable state may be the HS state. This is due to the fact that the entropy of the system in the HS state is much larger than in the LS state ( $\Delta S > 0$ ), and the gain is  $T\Delta S$ , where  $T$ , the temperature, compensates the energy loss. This LS  $\rightleftharpoons$  HS crossover can be thermally induced. When the process takes place in the solid state, it may be cooperative if the intersite interactions are strong enough. This cooperativity may lead to very abrupt transitions along with thermal hystereses. The thermal hysteresis width defines the temperature range of bistability for the system.<sup>2</sup> One of the main challenges is then to design spin-crossover compounds exhibiting large bistability range.

It has been suggested and experimentally confirmed that the cooperativity can be magnified by designing polymeric structures in which the active sites are linked to each other by chemical bridges. Some compounds of this kind have been found to display thermal hysteresis widths reaching ca. 40 K.<sup>3</sup> These polymeric compounds, however, are not strictly molecular any more. The question we were faced with was to see whether

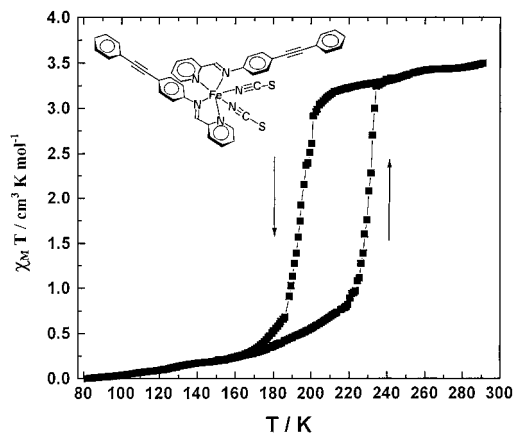


**Figure 1.**  $\chi_M T$  versus  $T$  plots for **1** in both cooling and warming modes. The temperature was varied at the rate of 1 K  $\text{min}^{-1}$  without overshooting. The sample consisted of about 20 mg of small single crystals.

purely molecular lattices consisting of spin-crossover mononuclear molecules could also exhibit wide thermal hysteresis loops. We report here on a compound of that kind, namely, *cis*-bis(thiocyanato)bis[*N*-(2'-pyridylmethylene)-4-(phenylethynyl)anilino]iron(II) (**1**). The absence of solvent molecule in the lattice eliminates the possibility of *apparent* hysteresis, resulting from the synergy between LS  $\rightarrow$  HS transformation and removal of noncoordinated solvent molecules,<sup>4</sup> as observed for instance for  $[\text{Fe}(2\text{-pic})_3]\text{Cl}_2 \cdot \text{H}_2\text{O}$  (2-pic = 2-picolyamine).<sup>5</sup>

The ligand *N*-(2'-pyridylmethylene)-4-(phenylethynyl)aniline,<sup>6</sup> noted hereafter as L, was prepared from 2-pyridinecarbaldehyde and 4-(phenylethynyl)aniline,<sup>7</sup> and the compound **1**<sup>8</sup> was synthesized under nitrogen by preparing first a solution of  $3.5 \times 10^{-4}$  mol of  $\text{Fe}(\text{NCS})_2$  in 50 mL of methanol (from the reaction of  $\text{Fe}(\text{SO}_4) \cdot 7\text{H}_2\text{O}$  with KNCS) and adding  $7 \times 10^{-4}$  mol of L in 50 mL of methanol.<sup>9</sup> Single crystals were obtained by slow diffusion of the two solutions in a H-shape tube.

The spin-crossover regime for a sample of **1** made of single crystals was investigated from the temperature dependence of  $\chi_M T$ , where  $\chi_M$  is the molar magnetic susceptibility and  $T$  is the temperature. At room temperature,  $\chi_M T$  is equal to  $3.5 \text{ cm}^3 \text{ K mol}^{-1}$ , which corresponds to what is expected for a HS state, decreases smoothly down to  $3.0 \text{ cm}^3 \text{ K mol}^{-1}$  as  $T$  is lowered down to 204 K, and then drops suddenly around  $T_{1/2} \downarrow = 194 \text{ K}$ . At 80 K,  $\chi_M T$  is close to zero. In the warming mode, the abrupt

(4) Garcia, Y.; van Koningsbruggen P. J.; Codjovi, E.; Lapouyade, R.; Kahn, O.; Rabardel, L. *J. Mater. Chem.* **1997**, *7*, 857.

(5) (a) Sorai, M.; Enslin, J.; Hasselbach, K. M.; Gütllich, P. *Chem. Phys. Lett.* **1980**, *74*, 3.  
 (b) Gütllich, P.; Köppen, H.; Steinhäuser, H. G. *Chem. Phys. Lett.* **1980**, *74*, 3.

(6) <sup>1</sup>H NMR ( $\text{CDCl}_3$ , 250 MHz)  $\delta$ : 8.8 (d, 1H), 8.6 (s, 1H), 8.2 (d, 1H), 7.9 (td, 1H), 7.7–7.3 (m, 10H, NH<sub>2</sub>). SM:  $m/e = 283$  ( $\text{MH}^+$ ). UV/vis ( $\text{CH}_3\text{CN}$ )  $\lambda_{\text{max}}$  (log  $\epsilon$ ): 293 (4.67), 339 (4.55).

(7) Synthesis of 4-(phenylethynyl)aniline: 0.5% mol of  $\text{PdCl}_2(\text{PPh}_3)_2$  and 0.5% mol of CuI were added to a carefully deoxygenated solution of phenylacetylene (2.33 g, 23 mmol) and 4-iodoaniline (5 g, 23 mmol) in diethylamine (50 mL). After 20 h at room temperature, the solvent was removed in vacuo and the solid was extracted with diethyl ether. Filtration, evaporation, and recrystallization from Et<sub>2</sub>O/pentane (1:3) gave pale yellow crystals (2.9 g, 67% isolated yield). <sup>1</sup>H NMR ( $\text{CDCl}_3$ , 300 MHz)  $\delta$ : 7.5 (m, 2H, Ph), 7.3 (m, 5H, Ph), 6.6 (m, 2H, Ph), 3.8 (br s, 2H, NH<sub>2</sub>). <sup>13</sup>C NMR ( $\text{CDCl}_3$ , 75 MHz)  $\delta$ : 146.74 (t, <sup>2</sup> $J_{\text{CH}} = 8.6 \text{ Hz}$ , C-NH<sub>2</sub>), 133.02 (dd, <sup>1</sup> $J_{\text{CH}} = 161 \text{ Hz}$ , <sup>2</sup> $J_{\text{CH}} = 6.5 \text{ Hz}$ ), 131.41 (dt, <sup>1</sup> $J_{\text{CH}} = 162 \text{ Hz}$ , <sup>2</sup> $J_{\text{CH}} = 6.3 \text{ Hz}$ ), 128.35 (dd, <sup>1</sup> $J_{\text{CH}} = 161 \text{ Hz}$ , <sup>2</sup> $J_{\text{CH}} = 7.5 \text{ Hz}$ ), 127.73 (dt, <sup>1</sup> $J_{\text{CH}} = 161 \text{ Hz}$ , <sup>2</sup> $J_{\text{CH}} = 7.5 \text{ Hz}$ ), 123.95 (t, <sup>2</sup> $J_{\text{CH}} = 7.2 \text{ Hz}$ ), 114.81 (dm, <sup>1</sup> $J_{\text{CH}} = 157 \text{ Hz}$ ), 112.61 (t, <sup>2</sup> $J_{\text{CH}} = 8.4 \text{ Hz}$ ), 90.22 (t, <sup>3</sup> $J_{\text{CH}} = 5.1 \text{ Hz}$ ), 87.41 (t, <sup>3</sup> $J_{\text{CH}} = 5.2 \text{ Hz}$ ).

(8) Anal. Calcd for  $\text{FeC}_{42}\text{H}_{28}\text{N}_6\text{S}_2$  (**1**): C, 68.48; H, 3.80; N, 11.41; S, 8.70; Fe, 7.61. Found: C, 68.78; H, 3.77; N, 11.14; S, 8.85; Fe, 7.60. IR (KBr,  $\text{cm}^{-1}$ ): 3054, 2060, 1592, 1502, 1441, 841, 758, 691. UV/vis ( $\text{CH}_3\text{CN}$ )  $\lambda_{\text{max}}$  (log  $\epsilon$ ): 283 (4.72), 335 (4.47), 591 (3.05).

(9) Létard, J.-F.; Montant, S.; Guionneau, P.; Martin, P.; Le Calvez, A.; Freysz, E.; Chasseau, D.; Lapouyade, R.; Kahn, O. *J. Chem. Soc., Chem. Commun.* **1997**, 745.

<sup>†</sup> Institut de Chimie de la Matière Condensée de Bordeaux.

<sup>‡</sup> Université de Rennes I.

(1) (a) Goodwin, H. A. *Coord. Chem. Rev.* **1976**, *18*, 293. (b) Gütllich, P. *Struct. Bonding (Berlin)* **1981**, *44*, 83. (c) Gütllich, P.; Hauser, A. *Coord. Chem. Rev.* **1990**, *97*, 1. (d) Gütllich, P.; Hauser, A.; Spiering, H. *Angew. Chem., Int. Ed. Engl.* **1994**, *33*, 2024 and references therein. (e) König, E. *Prog. Inorg. Chem.* **1987**, *35*, 527. (f) König, E. *Struct. Bonding (Berlin)* **1991**, *76*, 51.

(2) (a) Kahn, O.; Launay, J. P. *Chemtronics* **1988**, *3*, 140. (b) Zarembowitch, J.; Kahn, O. *New J. Chem.* **1991**, *15*, 181. (c) Kahn, O. *Molecular Magnetism*; VCH: New York, 1993.

(3) (a) Vreugdenhil, W.; van Diemen, J. H.; de Graaff, R. A. G.; Haasnoot, J. G.; Reegijk, J.; van der Kraan, A. M.; Kahn, O.; Zarembowitch, J. *Polyhedron* **1990**, *9*, 2971. (b) Kahn, O.; Kröber, J.; Jay, C. *Adv. Mater. Chem., Int. Ed. Engl.* **1994**, *33*, 2024 and references therein. (c) König, E. *Prog. Inorg. Chem.* **1987**, *35*, 527. (d) König, E. *Struct. Bonding (Berlin)* **1991**, *76*, 51. (e) Lavrenova, L. G.; Ikorskii, V. N.; Varnek, V. A.; Oglezneva, I. M.; Larionov, S. V. *Koord. Khim.* **1986**, *12*, 207. (f) Lavrenova, L. G.; Ikorskii, V. N.; Varnek, V. A.; Oglezneva, I. M.; Larionov, S. V. *Zh. Struk. Khim.* **1993**, *34*, 145. (g) Sugiyarto, K. H.; Goodwin, H. A. *Aust. J. Chem.* **1994**, *47*, 263. (h) Kröber, J.; Audière, J. P.; Claude, R.; Codjovi, E.; Kahn, O.; Haasnoot, J. G.; Grolrière, F.; Jay, C.; Bousseksou, A.; Linares, J.; Varret, F.; Gonthier-Vassal, A. *Chem. Mater.* **1994**, *6*, 1404. (i) Lavrenova, L. G.; Ikorskii, V. N.; Varnek, V. A.; Oglezneva, I. M.; Larionov, S. V. *Polyhedron* **1995**, *14*, 1333. (j) Kahn, O.; Codjovi, E.; Garcia, Y.; van Koningsbruggen, P. J.; Lapouyade, R.; Sommier, L. In *Molecule-Based Magnetic Materials*; Turnbull, M. M., Sugimoto, T., Thompson, L. K., Eds.; ACS Symposium Series 644; American Chemical Society: Washington, DC, 1996.

variation of  $\chi_M T$  was observed around  $T_{1/2}^\uparrow = 231$  K (Figure 1).  $T_{1/2}^\downarrow$  and  $T_{1/2}^\uparrow$  are defined as the inversion temperatures for which there are 50% of LS and 50% of HS molecules in the cooling and warming modes, respectively. Successive thermal cycles did not modify the thermal hysteresis loop. It was also checked that the shape of this loop did not depend on the rate of the temperature variation, provided that this rate is lower than  $1 \text{ K min}^{-1}$ .

The crystal structure of **1** was solved both at room temperature in the HS state and at 140 K in the LS state.<sup>10</sup> Those two structures are compared in Figure 2. The  $\text{LS} \rightleftharpoons \text{HS}$  crossover is accompanied by a crystallographic phase transition, between orthorhombic, *Pccn*, in the LS state and monoclinic, *P2<sub>1</sub>/c*, in the HS state. Quite unexpectedly, the symmetry of the low-temperature phase is higher than that of the high-temperature phase. The iron atoms are located on 2-fold symmetry axes in the LS state, while they are in general positions in the HS state. As expected, the Fe–N bond lengths are significantly shorter, and the  $\text{FeN}_6$  core is less distorted in the LS than in the HS state. Probably the key feature of the LS and HS structures lies in the presence of very short contacts ( $3.45 \text{ \AA}$  in both the LS and HS states) between phenyl rings belonging to adjacent molecules. Furthermore, the  $\text{Fe}(\text{NCS})_2$  linkage of each molecule is closely nested with the  $\text{FeL}_2$  linkage of an adjacent molecule along the *c*-axis in the LS state (*a*-axis in the HS state). The conjunction of this interlocking with the short contacts between phenyl rings confers a two-dimensional character to the structure in both the LS (*ac* planes) and HS (*ab* planes) states.

The  $\text{LS} \rightarrow \text{HS}$  crossover for **1** may also be induced optically at 10 K within the SQUID cavity through irradiation of a single crystal with the 528 nm line of a  $\text{Kr}^+$  laser coupled to an optical fiber (LIESST effect). The yield of the transformation, however, is far from being quantitative, in contrast with what was observed with the same equipment for  $[\text{Fe}(\text{ptrz})_6](\text{BF}_4)_2$  ( $\text{ptrz} = N$ -propyltetrazole), in full agreement with the original observations by Decurtins et al.<sup>11</sup> The total relaxation of the system from the HS to the LS state is above 70 K.

(10) Crystal data for  $\text{C}_{42}\text{H}_{26}\text{N}_6\text{S}_2\text{Fe}$ :  $M = 734$ ; at 293 K, monoclinic, space group *P2<sub>1</sub>/c* ( $Z = 4$ );  $a = 15.637(1) \text{ \AA}$ ,  $b = 14.566(8) \text{ \AA}$ ,  $c = 16.821(13) \text{ \AA}$ ;  $\alpha = 90^\circ$ ,  $\beta = 92.95(4)^\circ$ ,  $\gamma = 90^\circ$ ;  $V = 3826(4) \text{ \AA}^3$ ;  $D_c = 1.27$ ; Fe–N( $\text{CS}^-$ ) distances [Fe–N(2) =  $2.056 \text{ \AA}$  and Fe–N(5) =  $2.055 \text{ \AA}$ ]; Fe–N (organic ligand) distances [Fe–N(31) =  $2.164 \text{ \AA}$ , Fe–N(131) =  $2.167 \text{ \AA}$ , Fe–N(26) =  $2.246 \text{ \AA}$ , and Fe–N(126) =  $2.270 \text{ \AA}$ ]; at 140 K, orthorhombic, space group *Pccn* ( $Z = 8$ );  $a = 14.357(7) \text{ \AA}$ ,  $b = 14.291(6) \text{ \AA}$ ,  $c = 17.448(13) \text{ \AA}$ ;  $\alpha = 90^\circ$ ,  $\beta = 90^\circ$ ,  $\gamma = 90^\circ$ ;  $V = 3580(4) \text{ \AA}^3$ ;  $D_c = 1.36$ ; [Fe–N(2) =  $1.948(5) \text{ \AA}$ , Fe–N(31) =  $1.946(5) \text{ \AA}$ , and Fe–N(26) =  $1.971(5) \text{ \AA}$ ]; measurements were made with a Nonius CAD-4 diffractometer; Mo  $\text{K}\alpha$  ( $0.71069 \text{ \AA}$ ); crystal shape, black needles; Bragg angle  $\theta < 65^\circ$ ; empirical absorption correction  $0.926 < T < 1.000$ ; scan type,  $\omega/\theta$ ; at 293 K (140 K) 5446 (5474) measured reflections, 2318 (1381) observed [ $I > 3\sigma(I)$ ]; structural determination with MITHRIL package and structural refinement with SHELX93; at 293 K (140 K) 460 (230) parameters;  $R = 5.4\%$  (4.0);  $R_w = 5.4\%$  (4.1). The temperature-dependent single-crystal X-ray analyses show that Fe–N( $\text{CS}^-$ ) bond lengths are shortened by about 5% and Fe–N(organic) are by 10%, which corresponds to 3% of the unit cell volume (change of  $100 \text{ \AA}^3$ ).

(11) Decurtins, S.; Gütllich, P.; Köhler, C. P.; Spiering, H.; Hauser, A. *Chem. Phys. Lett.* **1984**, *105*, 1.

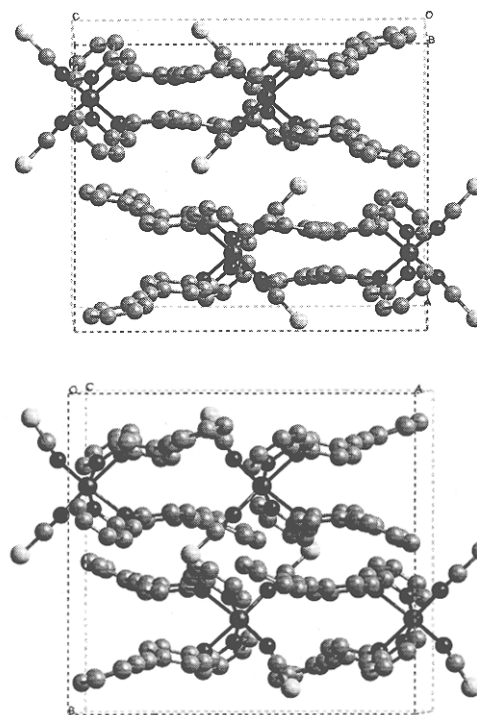


**Figure 2.** Molecular structure in the LS (140 K) and HS (293 K) states. (Top) Projection of the LS form along the *b*-axis. The shortest iron–iron separation is  $8.73 \text{ \AA}$  (along the *c*-axis). (Bottom) Projection of the HS form along the *c*-axis. The shortest iron–iron separation is  $8.49 \text{ \AA}$  (along the *a*-axis).

Let us mention that a similar compound,  $\text{FeL}_2(\text{NCSe})_2$ ,<sup>12</sup> in which  $\text{NCSe}^-$  replaces  $\text{NCS}^-$ , was also synthesized. This compound shows a wide hysteresis loop with  $T_{1/2}^\downarrow = 256 \text{ K}$  and  $T_{1/2}^\uparrow = 306 \text{ K}$  (on a powder sample). Room temperature falls within the hysteresis loop.

The title compound, to the best of our knowledge, is the mononuclear spin crossover species exhibiting the widest thermal hysteresis loop ( $37 \text{ K}$ ), reproducible over successive thermal cycles, reported so far.<sup>13</sup> The cooperativity may be attributed to both intermolecular  $\pi$  interactions between phenyl rings and interlocking of the molecular units.

**Supporting Information Available:** Tables giving crystallographic data, positional parameters, and  $U$  values (10 pages). See any current masthead page for ordering and Internet access instructions.

JA972441X

(12) Anal. Calcd for  $\text{Fe}(\text{L})_2(\text{NCSe})_2$ ,  $\text{FeC}_{42}\text{H}_{28}\text{N}_6\text{Se}_2$ : C, 60.72; H, 3.37; N, 10.12; Se, 19.04; Fe, 6.75. Found: C, 60.64; H, 3.30; N, 9.68; Se, 18.84; Fe, 6.76.

(13) For instance, see: (a) Ritter, G.; König, E.; Irlner, W.; Goodwin, H. A. *Inorg. Chem.* **1978**, *17* (2), 224. (b) König, E.; Ritter, G.; Kulshreshtha, S. K. *Chem. Rev.* **1985**, *85*, 219. (c) Bradley, G.; McKee, V.; Nelson, S. M. *J. Chem. Soc., Dalton Trans.* **1978**, 522.